FEEDBACK AND FEEDFORWARD VIBRATION CONTROL STRATEGY FOR SYNCHRONOUS DISTURBANCES IN A ROTOR WITH ERROR SENSORS IN OPTIMAL LOCATIONS

Efrain Araujo Perini, eaperini@ipen.br
Luiz de Paula do Nascimento, depaula@dem.feis.unesp.br
Sao Paulo State University, Ilha Solteira, Brazil

Abstract. *This work investigates a theoretical study of the error sensor placement in a rotor controlled with the feedforward technique associated with the feedback technique using magnetic actuators. The results are calculated based on the LMS (Least Mean Square) x-filtered algorithm, which is a numerical solution for modeling the feedforward adaptive control, widely used in vibration and acoustic control, whereas here is used for attenuating rotors vibrations levels in synchronous and sub-synchronous disturbances. The research starts with a rotor model that work levitated using two magnetic actuators for levitation and vibration control purposes, simultaneously, associating feedback and feedforward control strategies. Also, this work focuses on the control force, global and local vibrations along the rotor, considering the actuator design limitations for the control requirements to this unbalanced rotor model system.*

Keywords*: synchronous vibration, feedforward control, magnetic bearing, error sensors*

1. INTRODUCTION

Active magnetic bearings (AMBs), which support rotors or shafts without any mechanical contact or lubrication by electromagnetic forces, are nowadays widely used in high-speed turbomachinery and precision machinery. AMBs offer some important advantages over conventional ball or roller bearings, such as no contact between bearings, and consequently, no need for lubricants, which makes them very useful in special high temperature or vacuum environments. On the other hand, it is difficult to design active controls for magnetic bearings systems because of their high nonlinearity and open-loop unstable electromagnetic dynamics (Chen *et al*., 2009). In recent years, several nonlinear control techniques have been proposed as in Behal *et al*. (2001), in Lévine *et al.* (1996) and in Queiroz and Dawson (1996), for AMB systems including sliding mode (Torres *et al.*, 1999), feedback linearization (Smith and Weldon, 1995) and hybrid control (Al-Holou *et al.*, 2002), all designed to improve their disturbance rejection properties and robustness in terms of unmodeled dynamics and parameter uncertainties. Although magnetic bearing systems are inherently reliable, a significant issue in the design of magnetic bearing systems for both current and potential machine applications is improvement of fault tolerance. Cole *at al.* (2004) stated that failure of a single system component can give rise to destructive rotor dynamic behaviour, particularly if the rotor is not constrained effectively by auxiliary bearings. The issue of actively controlling the non-linear dynamic response of the rotor when interaction with auxiliary bearings occurs is an important aspect of fault tolerance. One requirement for achieving this tolerance is that system stability can be conserved during a fault condition. In addition, there may be performance requirements to ensure, for example, safe rotor run-down through critical speeds. Selection of bearing and sensor configuration is an important role in the fault tolerance and vibration control. However, there is a strong argument for achieving better system performances with the minimum system complexity. In this context, some rotors may require increased seal clearances to achieve satisfactory operation, from the stability point of view, with a consequent decrease on efficiency. The development of a reliable technique to damp sub-synchronous vibration could reduce or eliminate this trade-off, resulting in the design of more efficient machinery.

In Figure 1 is shown one quadrant of a radial AMB consisting of a position sensor, a controller, a power amplifier and an electromagnetic actuator. For operation, the sensor measures the position of the shaft and the measured signal (x_s) is sent to the controller where it is processed and then, the signal is amplified and fed as a current (i_p) into the coils of the magnet, generating an electromagnetic field that keeps the shaft in a desired position. The strength of magnetic field depends on the air gap between the shaft and the magnet and the dynamics of the system including the design of the controller.

Control technology has made possible the use of AMBs to adjust the dynamics (stiffness and damping) of a rotor system, based on constant monitoring of the position of the shaft, this fact has introduced the concept of Active Magnetic Dampers (AMD), which no static load capacity is placed in a machine for vibration control purposes. The AMB modeling with the PID feedback control was developed with basis on Maslen (2000). Therefore, this paper brings an AMB modeling associated with the feedforward control over the feedback control inherent to the AMB system to analyze the effect of actuator and sensor placement on the active vibrations control of rotor unbalance focusing on synchronous and subsynchronous vibrations and also contributes to the adaptive control performance investigation that uses the LMS X-filtered algorithm. More information about this technique and rotor modeling can be found in Johnson

et al. (2003), which investigates this control strategy theoretically and numerically without investigating synchronous and subsynchronous vibrations control.

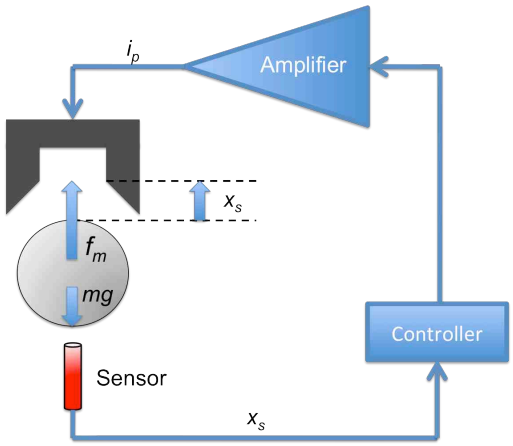

Figure 1. Basic geometric configuration of a double action radial magnetic bearing.

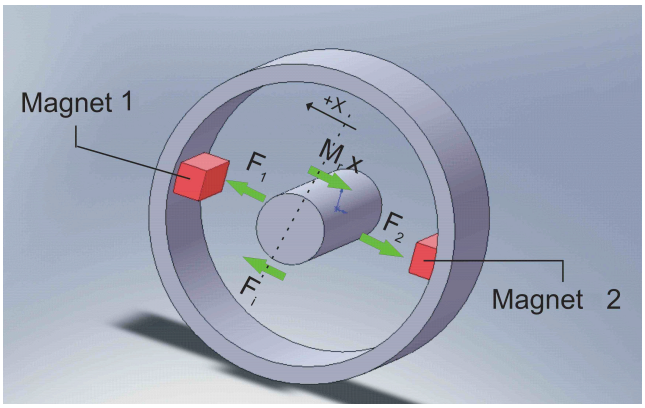

Figure 2. Layout of a controlled shaft using a radial magnetic bearing.

2. AMB THEORY CONCEPT

Active Magnetic Bearing (AMB) theory is deeply linked with electromagnetism science and the study of its theory is the bottom line in developing a MMA rotor system modeling. In analyzing the behavior of a magnetic actuator, the primary objective is to determine the forces generated by the actuator in response to voltages applied to its coils and motion of the actuated device. Once this analysis is well established, it can be used in the design of actuators to provide the effects of the various design parameters and latter be used to evaluate design choices (Maslen, 2000).

The analysis of the coil/geometry – force relationship and of the electrical properties is generally done using a fairly simple one–dimensional representation of the magnetic structure of the actuator. This approach is referred to as magnetic circuit analysis. It is known that the magnetic flux is generated in each pole of the actuator by a rolling up of N coils with an electrical current passing through it. It is good to highlight that in a magnetic bearing effects like forces lines diffusion and current flight are generally not taken into account in the electromagnetic force equation. Therefore, a geometric correction factor ε can conventionally be used to provide more precise results by taking into consideration these effects. Thus, from the magnetism physics principles, the force equation that the AMB can act in function of its geometric and build parameters can be reached, according to [16] is,

$$F = \varepsilon \frac{\mu_0 N^2 i^2 A_g}{4g^2} \tag{1}$$

where $\mu_0 = 4\pi x 10^{-7} (Hm^{-1})$ is the permeability of the free space (air), g is the gap between the rotor and the stator, A_g is the area face of each pole and the geometric correction factor ε is evaluated as 0.9 for axial bearing and 0.8 for radial bearing. These numbers are due to the electrical current flight effect and it is more accentuated in bearings with radial geometry. Once the electromagnetic forces are only of attraction, the actuator must be positioned in both sides and diameterly opposite from the rotor, in a double action scheme, as shown in Figure 2, in a manner that the net force F_N in the bearing plane is given by

$$F_N = F_2 - F_1 = K_i i_p - K_x x_i \tag{2}$$

where K_i is the current stiffness, K_x is the position stiffness, i_p is the control current and x_i is the shaft displacement.

In Figure 2, F_1 and F_2 are attraction forces that act in one control axis, F_i is a harmonic external force applied upon the system and M_r is the rotor differential mass.

3. THE X-LMS ALGORITHM THEORY

The X-LMS algorithm is briefly described and then is applied in a one-dimensional model of a rotor to investigate the performance of an active control system. The model of this work is based on a beam model (i.e. does not take in account the gyroscopic effects) and is intended to act as a tool by witch the actuator and sensor locations can be investigated. Detailed information about the X-LMS algorithm can be found in Elliot *et al.* (1987).

The filtered X-LMS is a time domain algorithm that uses a reference signal x to drive a set of secondary actuators in order to affect the system under control. As can be seen in Figure 3, the reference signal is first digitally sampled and then passed through a finite impulse response (FIR) control filter *W* before being converted back into an analog signal *y* used to drive the actuator to control the plant *G*. Another set of sensors, called error sensors, is used to monitor the behavior of the system (error *e*) and is used to automatically adapt the control FIR filter using the LMS algorithm. The plant represents the transfer function between the input to the actuators (magnetic bearing currents in this case) and the vibration detected at the error sensors. The disturbance *d* is the vibration at the error sensors due to the unbalance in the system. This control architecture differs from the LMS in that the reference signal needs to be first filtered by a model of the plant *G* (i.e. filtered-*x*) before being used by the LMS algorithm. The model of the plant is usually stored as an FIR filter and is measured in a system identification stage before the control system is turned on.

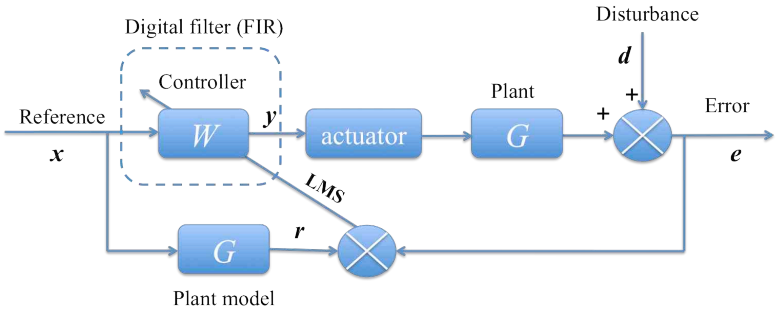

Figure 3. Block diagram for the filtered-x LMS adaptive control system.

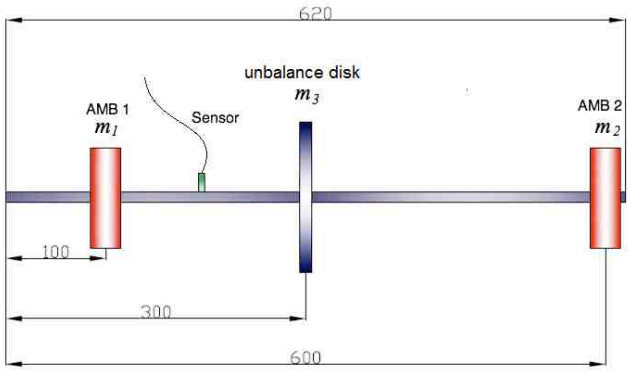

Figure 4. Schematic of rotor system model

If a signal has been sampled at a discrete time interval then it can be considered as a sequence x(n) where n can only take integer values. The current output of an FIR filter, such a W, is the weighted sum of the previous inputs. The LMS algorithm updates the filter coefficients in W using the most recent error signal e(n) and the past I filtered reference signals r(n-i).

$$w_i(n+1) = w_i(n) - \alpha e(n) r(n-i) \tag{3}$$

All I filter coefficients can be updated this way. The coefficient α is the convergence coefficient and determines how rapidly the control system converges. α must be large enough such that the convergence time is small but cannot be too large since this can cause instability. Ideally, this algorithm converges to a solution where the time average sum of the squared error signals is minimized. In principle, only 2 coefficients are necessary to achieve good control if the disturbance is at a single frequency. If multiple frequencies need to be controlled, for example harmonics of the rotor speed, then more than two coefficients are necessary (Johnson *et al.*, 2003).

4. RORROR MODEL FOR ACTIVE CONTROL ANALIZIS

The rotor will be considered as a free beam with gyroscopic effects neglected with masses attached and supported by bearing modeled as a pair of springs and dampers, the unbalance and control forces and have been introduced onto the beam to determine the optimal active control performance. Only the vertical velocity will be considered in this model.

The model used can be found in Johnson *et al.* (2003), where it defines the transfer mobility $\mathbf{T_{ij}}$ as the velocity of the bean at position $\mathbf{x_i}$ due to an input force at position $\mathbf{x_j}$. At a single frequency, the velocities at a number of locations can be described in matrix form as,

$$\mathbf{u_i} = \mathbf{T_{ij}}\mathbf{f_j} \tag{4}$$

where the column vector $\mathbf{u_i}$ describes the velocities at positions $\mathbf{x_i}$ (also column vector) due to a number of forces $\mathbf{f_j}$ acting at locations $\mathbf{x_j}$. Each element in the matrix $\mathbf{T_{ij}}$ is calculated using the transfer mobility equation.

The bearing stiffness, damping or mass will be added to the model using the matrix impedance method (Bishop and Johnson, 1960). As shown in Figure 4, the rotor interacts with external loads at three points along the beam: two active magnetic bearings (m_1 and m_2) and one unbalance disk (m_3).

In the AMB positions, the rotor is supported by two virtual springs of stiffness k_1 and k_2 and in the middle of the beam where a mass m_3, containing a slight unbalance, is applied. The bearings are also considered to have viscous dampers c_1 and c_2 included in them. The mass and stiffness attachments create reaction forces when the rotor is moved and these forces can be described using an impedance matrix $\mathbf{Z}$ as it follows,

$$\mathbf{f_r} = -Zu_m \Leftrightarrow \begin{bmatrix} f_{r1} \\ f_{r2} \\ f_{r3} \end{bmatrix} = \begin{bmatrix} j\omega m_1 + c_1 + \dfrac{k_1}{j\omega} & 0 & 0 \\ 0 & j\omega m_2 + c_2 + \dfrac{k_2}{j\omega} & 0 \\ 0 & 0 & j\omega m_3 \end{bmatrix} \begin{bmatrix} u_{m1} \\ u_{m2} \\ u_{m3} \end{bmatrix} \tag{5}$$

where $\mathbf{u_m}$ is the vector of velocities at the three mass locations and the reaction force is given by the vector $\mathbf{f_r}$. The velocity vector um can be considered as the combination of the velocity $\mathbf{u_{mr}}$ due to the reaction forces $\mathbf{f_r}$ and the velocity $\mathbf{u_{mj}}$ due to external input forces in this model created by the mass unbalance and by the active control forces. The expression of the reaction force in terms of the external forces can be written as

$$\mathbf{f_r} = -\mathbf{Z}\mathbf{u_m} = -\mathbf{Z}\left[\mathbf{I} + \mathbf{T_{mm}}\mathbf{Z}\right]^{-1}\mathbf{T_{mj}}\mathbf{f_j} \tag{6}$$

The matrices $\mathbf{T_{mm}}$ and $\mathbf{T_{mj}}$ contain rotor mobilities describing the velocity at the three locations due to forces acting at the mass locations and the locations of the external forces respectively. The mobility equation (Equation 4) including reaction forces can be written as

$$\begin{aligned} \mathbf{u_i} &= \mathbf{T_{ij}}\mathbf{f_j} + \mathbf{T_{im}}\mathbf{f_r} = \hat{\mathbf{T}}_{\mathbf{ij}}\mathbf{f_j} \\ \hat{\mathbf{T}}_{\mathbf{ij}} &= \left[\mathbf{T_{ij}} - \mathbf{T_{im}}\mathbf{Z}\left[\mathbf{I} + \mathbf{T_{mm}}\mathbf{Z}\right]^{-1}\mathbf{T_{mj}}\right] \end{aligned} \tag{7}$$

The matrices $\mathbf{T_{im}}$ and $\mathbf{T_{ij}}$ contain rotor mobilities describing the velocity at the observation locations $\mathbf{x_i}$ due to forces acting at the mass locations and at the locations of the external forces. With this, the vibration attenuation achieved with the control strategy can be analyzed.

5. ACTIVE CONTROL STRATEGY

Both feedback and feedforward strategies can be used for vibrations attenuation in magnetic bearing systems. In this work the filtered-x least mean square (LMS) adaptive filter algorithm from Widrow and Stearns (1985) is used measuring the de rotor displacement as the nulling error. This adaptive algorithm is implemented together with a basic PID feedback controller stabilizing the bearing system, as shown in Figure 5.

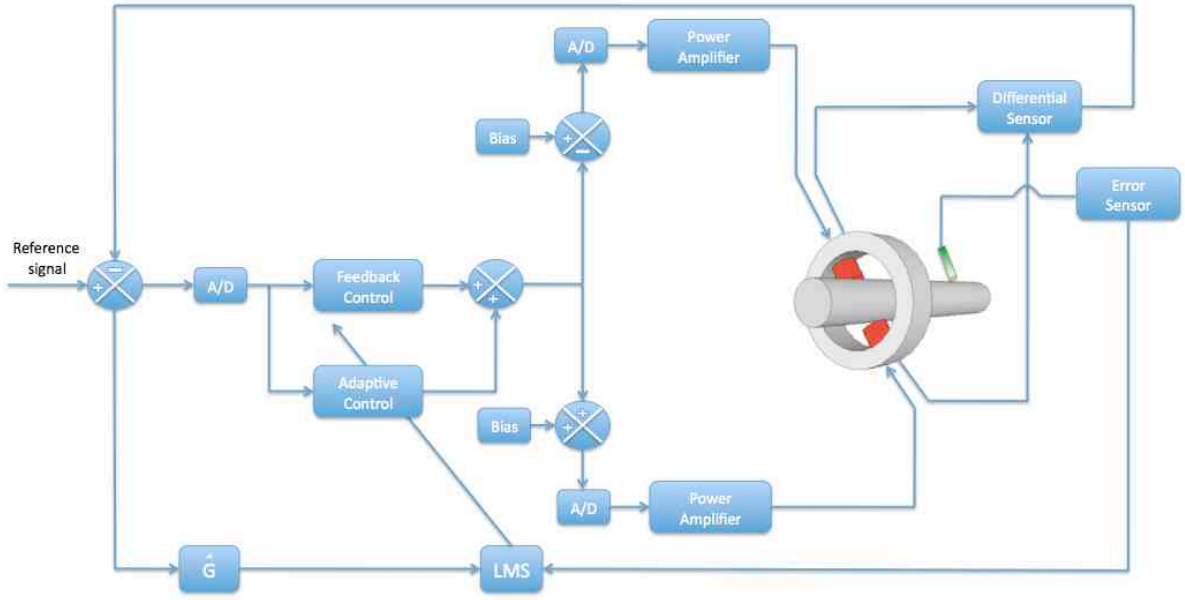

Figure 5. Feedforward associated with feedback control strategy for the magnetic actuator system.

If the feedforward system has J control actuators and L error sensors then at a single frequency the L length vector of errors (error sensors) $\mathbf{e}$ can be written in terms of the vector of primary disturbance forces $\mathbf{f_p}$ (rotor unbalance) and the J length vector of secondary control forces $\mathbf{f_e}$.

$$\mathbf{e} = \hat{\mathbf{T}}_{\mathbf{ep}}\mathbf{f}_{\mathbf{p}} + \hat{\mathbf{T}}_{\mathbf{ec}}\mathbf{f}_{\mathbf{c}} \tag{8}$$

The matrices $\hat{\mathbf{T}}_{\mathbf{ep}}$ and $\hat{\mathbf{T}}_{\mathbf{ec}}$ contain augmented rotor mobility describing the velocity at the error locations $\mathbf{x_e}$ due to forces acting at the locations $\mathbf{x_p}$ of the unbalance forces and the locations $\mathbf{x_c}$ of the control forces. The sum of the squared error signals can be calculated using the Hermitian transposed (or conjugate transposed denoted by $^{\mathbf{H}}$) as $\mathbf{e}^{\mathbf{H}}\mathbf{e}$ and is minimized when the secondary control forces $\mathbf{f_c}$ are given by [20],

$$\mathbf{f}_{\mathbf{c\_opt}} = \left[\hat{\mathbf{T}}_{\mathbf{ec}}^{\mathbf{H}}\hat{\mathbf{T}}_{\mathbf{ec}}\right]^{-1}\hat{\mathbf{T}}_{\mathbf{ec}}^{\mathbf{H}}\hat{\mathbf{T}}_{\mathbf{ep}}\mathbf{f}_{\mathbf{p}} \tag{9}$$

Using this optimal forces, the velocity at any observation position $\mathbf{x_i}$ can be calculated before $\mathbf{u_{i\_b}}$ and after $\mathbf{u_{i\_a}}$ optimal control as,

$$\mathbf{u}_{\mathbf{i\_b}} = \hat{\mathbf{T}}_{\mathbf{ip}}\mathbf{f}_{\mathbf{p}} \tag{10}$$

$$\mathbf{u}_{\mathbf{i\_a}} = \hat{\mathbf{T}}_{\mathbf{ip}}\mathbf{f}_{\mathbf{p}} + \hat{\mathbf{T}}_{\mathbf{ic}}\mathbf{f}_{\mathbf{c\_opt}} \tag{11}$$

The matrices $\hat{\mathbf{T}}_{\mathbf{ip}}$ and $\hat{\mathbf{T}}_{\mathbf{ic}}$ contain augmented rotor mobility describing the velocity at the observation locations $\mathbf{x_i}$ due to forces acting at the locations $\mathbf{x_p}$ of the unbalance forces and the locations $\mathbf{x_c}$ of the control forces. This process is frequency dependent and can be repeated for a range of sampling frequencies.

6. THEORETICAL ANALIZYS

6.1. Actuator selection

The performance of the control system implemented on the models shown in Figure 4 will be limited by the control architecture, the actuator placement and the sensors quantity and their arrangement. However, the control performance will be evaluated by the RMS vibration attenuation in synchronous frequency and also by the control force monitoring. The AMBs structural parameters for this model can be found in Table 1.

Basically, as shown in Figure 4, this research work proposes one theoretical steal rotor (Elastic or Young Modulus (E) of 209 GN/m^2, density of 7,800Kg/m^3, structural damping ratio (ξ) of 0.001) with a shaft of 620 mm long, 12 mm diameter, supported by two active magnetic bearings (AMBs). These systems are unbalanced with a single rigid steal disk of 0.5 Kg (m_3), diameter of 150 mm, thickness of 11 mm and eccentricity (e) of 0.11 mm, thus, the system unbalance characteristic is $m_3 \times e = 5.5\ 10^{-5}$ kg.m. In the model in study, one AMB is positioned at 100 mm from the left shaft endpoint and the second AMB at 20 mm before the right shaft endpoint. The first critical frequency of this rotor model is found at 34 Hz and, the damping added to the system from the two AMBs caused a high attenuation on low frequencies vibration amplitudes, thus the following critical frequency is observed at 338 Hz. The rotor is considered to operate at 4800 rpm, which means the subsynchronous and synchronous frequencies were set at 40 Hz and 80 Hz, respectively in a way to let those disturbances relatively close to the first critical speed. Fig. 6 shows the frequency response of this model operating under the feedback control only, i.e. feedforward control off (Ff Control off).

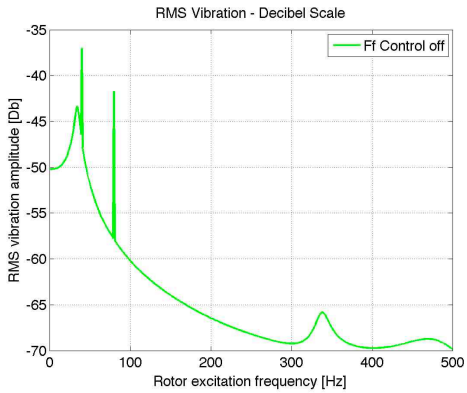

Figure 6. Frequency response of the rotor model with the subsynchronous (40 Hz) and synchronous (80 Hz) disturbances and with the feedforward control off (Ff Control off).

Table 1. Design parameters of the AMBs under analysis

Parameter	Value
ε (geometric correction factor)	0.8
μ_0 (permeability of the free space (air))	4π x 10^{-7} Hm^{-1}
A_g (gap area between the rotor and the stator)	67.558 x 10^6m^2
N (number of coils)	228
i (saturation electrical current)	3.0 A
i_b (permanent electrical current)	1.5 A
g_0 (gap between the rotor and the stator)	3.81 x 10^{-4}m
SS (displacement sensor sensitivity)	2.437 V/m
F (Maximum control force)	53 N
m_1 and m_2 (magnetic bearing mass)	0.250 kg
K_D *(PID controller derivative gain)*	0.3
K_I *(PID controller integral gain)*	80
K_P *(PID controller proportional gain)*	60
K_T *(PID controller total gain)*	0.00006

Once this model satisfies the AMB design specifications under the feedback control only, the first analysis lays on to decide which AMB will be the actuator and witch one will operate just as an active damper (Active Magnetic Damper – AMD) when the feedforward control is switched on. Thus, a theoretical model is designed by numerically placing one error sensor in each rotor node and then three cases of control performance are analyzed: both AMBs (AMB#1 and AMB#2) as actuators, AMB#1 as actuator, and then AMB#2 as actuator only. The results are shown in Figure 7.

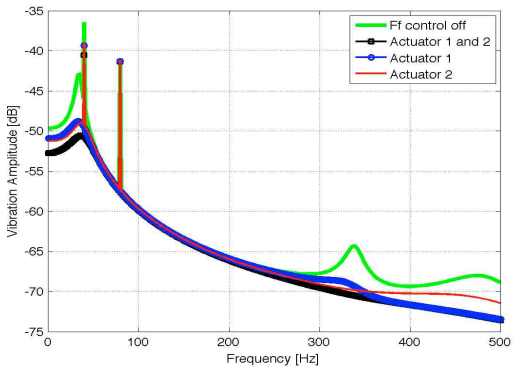

Actuator	Subsynchronous RMS attenuation (%)	Synchronous RMS attenuation (%)
AMB#1 and AMB#2	60.87	4.66
AMB#1	48.82	4.13
AMB#1	44.58	0.50

Figure 7. AMB selection from the rotor theoretical model.

As shown in Figure 7, the two actuators arrangement provides a better performance to the control system for both systems. However, from the SISO and MIMO active control theory (Fuller *et al.*, 1996), a single channel active control system is able to control vibrations in one direction, in a single point in a certain structure however, to control more than one point and direction, it is necessary to use multiple actuators to control the vibrations measurements from multiple (error) sensors. Thus, for one sensor case, AMB#1 is chosen for the feedforward control and, for two or more sensors cases, AMB#1 and AMB#2 are chosen to operate simultaneously on the feedforward control.

6.2. Subsynchronous and synchronous vibrations study

The rotor in study was investigated under the cases of one, two and three error sensors. Since three sensor demand higher computational and financial costs, this sensors limit number was stipulated. A computational code numerically searched the optimal sensors arrangement in order to provide the system with the lowest RMS vibrations on synchronous and subsynchronous frequencies. Results for the rotor operating at 4800 rpm can be seen in Fig. 8. It is worth to mention that no design parameters of AMB#1 neither of AMB#2 were saturated with sensors arrangement.

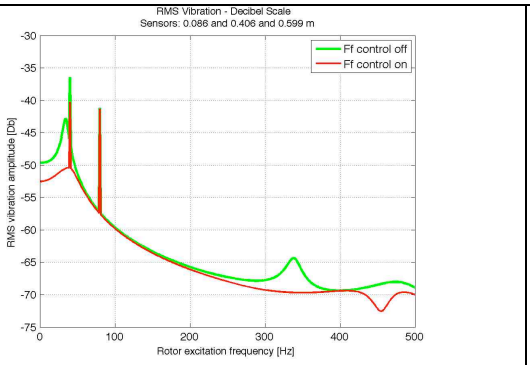

RMS attenuation (%)	
Subsynchronous	**Synchronous**
58.32	4.68
Sensors optimal placement (m):	
0.086; 0.406 e 0.599	

Figure 8. Frequency response and results for the rotor model with three error sensors placed in the optimal positions along the shaft.

In order to investigate the RMS vibrations attenuation performance (Fig. 8), the rotor model local vibrations in subsynchronous (40 Hz) and synchronous (80 Hz) frequencies are shown in Fig. 9.

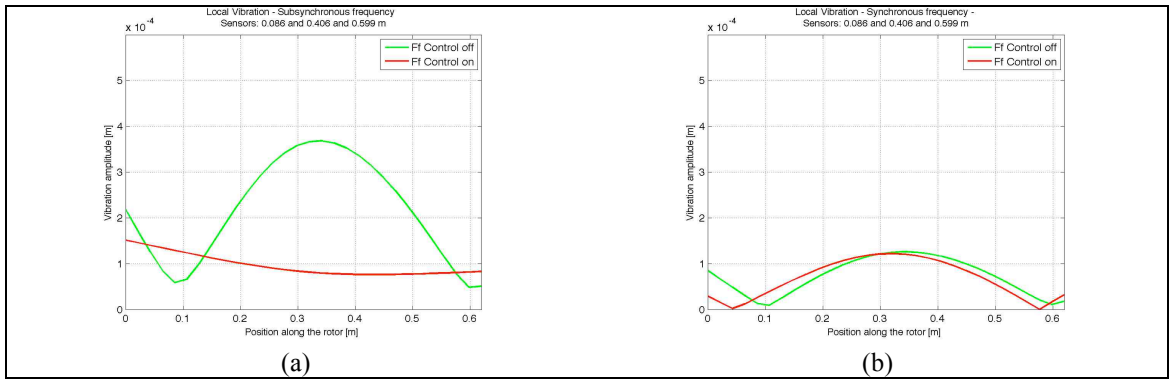

(a) (b)

Figure 9. Local vibrations along the model shaft with three error sensors for the feedforward control in (a) subsynchronous and (b) synchronous frequencies.

The values of control current, control magnetic force and shaft displacement on the AMBs nodes can be seen on Tab. 2. Those values represent the control effort on each AMB, and displays that no design parameters were saturated and neither the AMB gap (3.81 x 10^{-4}m) was overlapped by the shaft displacement as well.

Table 2. Control effort parameters on each AMB.

	Frequency	Control current (A)	Control magnetic force (N)	Shaft displacement at the AMB node (m)
AMB#1	Subsynchronous	1.145	32.334	1.253E-04
	Synchronous	0.533	17.479	3.458E-05
AMB#2	Subsynchronous	0.747	21.118	8.184E-05
	Synchronous	0.263	8.638	1.709E-05

Finally, for the sensors optimal arrangement allocation, the control current behavior for the RMS vibration attenuation was investigated in a synchronous frequencies range from 0 to 1200 Hz. Fig. 11 brigs the plots of this study where it is possible to see the great reductions (disregard to the AMBs design parameters saturations) happen with derivative gain 0.1 (k_d , from the AMB feedback control system).

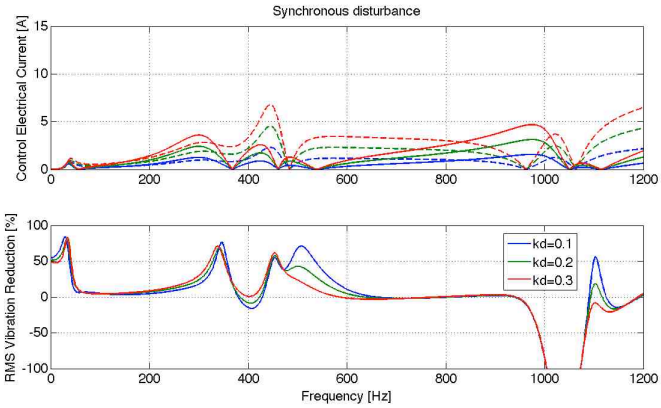

Figure 10. Control current (A) and RMS vibration reduction (%) behaviour in a range of synchronous frequency for AMB#1 (dashed line) and AMB#2 (solid line).

From Figure 10, it can be concluded that some frequency ranges has better reductions for the reason of the system behavior itself, since the critical frequencies change in function of k_d, and, as it is known, vibrations control are easily reached in the critical frequency range. In this way, Fig. 10 plots show that high levels attenuations are not necessarily reached with high electrical current magnitudes, once some control system parameters can change the dynamic system behavior and, in the same context, out of the critical frequencies vicinity it states low control system performance with some high electrical current levels. For the three sensors case, it can be observed that some electrical current peaks (what features system instabilities) do not happen and the maximum vibrations attenuations have more than 50%, which are higher than the maximum attenuation reached in the system with one or two error sensors. It its worth to highlight that this control system, in particular, states considerable vibrations controls in the first critical frequency vicinity and, for the frequencies higher than 338 Hz, the different values for k_d leads considerable and different vibrations reductions in the critical frequencies surroundings. Also, it needs to be mentioned that the three sensors case required the lowest electrical current levels in this whole frequency range, stating the best control performance for this system, especially when it comes to control the vibrations in the first critical frequency.

6.3. Feedback and feedforward control system comparison for subsynchronous and synchronous vibrations

In previous research works (Perini and Nascimento, 2008) a theoretical analysis was carried out with a system similar to this rotor model in study to investigate how subsynchronous and synchronous vibrations are attenuated in function of the AMB position. However, two conventional (contact) bearings were used to shaft support instead of AMBs for levitation. Therefore, with the AMB in the best location (close to the unbalanced mass), that previous system vibrations attenuations can be compared with this levitated model results, since the mechanical system design is still the same despite the conventional bearing replacement to the magnetic bearings. When comparing the prior system frequency response to the actual system response (yet with the feedforward control off), it can be seem a highly damping level, once all the low critical frequencies were completely attenuated (see Fig. 11). When the feedforward control is switched on, higher attenuations on the critical frequencies levels are observed, although the vibrations amplitude out of the critical frequencies surroundings are not relevantly attenuated. Those comparisons can be checked in the following Fig. 11.

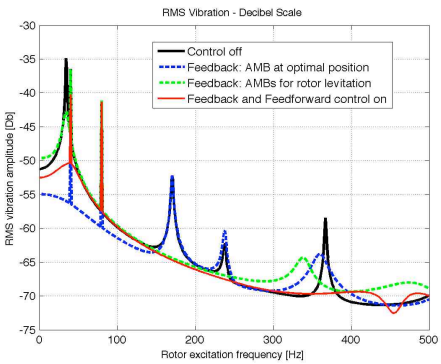

Figure 11. Frequency response comparisson to the different control systems applied to similar rotor models.

Table 3 brings subsynchronous and synchronous vibrations attenuations for each active control case in study. For the same cases, local vibrations through the shaft are shown in Figure 12 and the control force on each AMB can be found in Tab. 4.

Table 3. Vibrations reductions reached in 40 Hz (subsynchronous) and 80 Hz (synchronous) frequencies for each active control case.

Case	Subsynchronous RMS attenuation (%)	Synchronous RMS attenuation (%)
Feedback: AMB at the optimal position (conventional bearing for rotor support)	89,38	40,76
Feedback: AMB only for rotor levitation (feedforward off)	8,52	4,29
Feedback and feedforward simultaneously	61,87	8,77

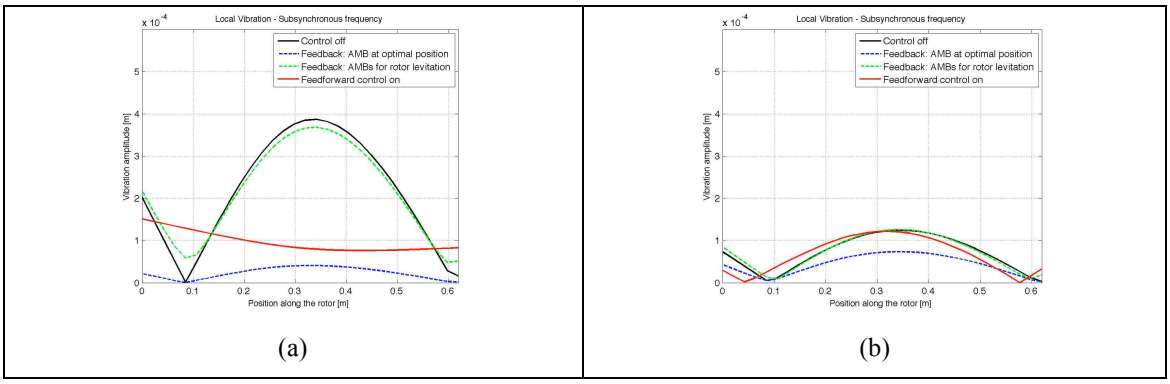

Figure 12. Comparison of local vibration though the shaft in the subsynchronous (40 Hz) and synchronous (80 Hz) frequencies for each active control case.

Table 4. AMBs control force in 40 Hz (subsynchronous) and 80 Hz (synchronous) frequencies for each active control case.

	Frequency	Feedback: AMB at the optimal position	Feedback: AMB only for rotor levitation	Feedback and feedforward simultaneously
AMB#1	Subsynchronous	10,524	15,358	32,334
	Synchronous	36,869	3,273	17,479
AMB#2	Subsynchronous	(no AMB#2)	12,258	21,118
	Synchronous	(no AMB#2)	5,353	8,638

It is worth to highlight that those results are for the rotor speeds in 40 Hz (subsynchronous) and 80 Hz (synchronous) and, in general, higher control force levels are required in the AMBs when they are working under feedforward control than under only the feedback control with the actuator in the optimal position.

7. CONCLUSIONS

The theoretical rotor model in study was proposed to investigate the feedback and feedforward active control techniques in order to specify each control performance for subsynchronous and synchronous disturbances. For the feedback control case only, it is possible to reach great reductions for RMS and local vibrations by allocating the AMB in the optimal position, that is close to the unbalance mass, which is the excitation forces source in the rotor. However, for cases when it is not possible to control high frequencies vibrations and high vibration modes (Perini and Nascimento, 2008) or even when it is not physically possible to allocate the AMB in the optimal position to apply feedback control, it becomes necessary to make use of the feedforward control strategy, which focus on the vibrations attenuations where the error sensors are placed.

From the methodology and control strategies used in this study, we conclude that is necessary to carry out the actuator selection analysis before proceed with the feedforward control application, once for example, one actuator and one error sensor were enough for relevant attenuations of deterministic vibrations close to the first critical frequency. Although, from the modal responses analyzed in this study, the two actuators and three error sensors control architecture resulted in a better vibrations control performance with no system instabilities in the whole frequency range analyzed. Thus, the actuators and sensors quantification in a rotating machine is conditional to the operation speed and, consequently, to its modal response. When the analysis comes to the error sensor allocation, the computational codes recommend placing each of them close to both actuators and other close to the unbalance mass.

Finally, contributing to the work of Johnson et al. (2003) regarding to the synchronous and subsynchronous vibrations control, it is concluded that deterministic perturbations attenuations is hardly reached with a simple control strategy, what can involve several sensors and actuators or even indirect methods to calculate the errors to be minimized in the feedforward strategy, as done by Shi et al. (2004). This work also takes a close look at the electrical control current and the control force, which are important measurements to track in order to avoid those limited design parameters to saturate at each AMB. In the same sense, it is also important to track the maximum rotor displacement at the AMBs nodes to avoid the contact (or structural damage) between rotor and the actuators stators.

8. ACKNOWLEDGEMENTS

The authors thank São Paulo State Research Council (FAPESP-Brazil), INCT-EIE, CNPq and FAPEMIG to support this work research.

9. REFERENCES

Al-Holou, N., Lahdhiri, T., Joo, D. S., Weaver, J., & Al-Abbas, F., Sliding mode neural network inference fuzzy logic control for active suspension systems. IEEE Transactions.

Behal, A., Costic, B. T., Dawson, D. M., & Fang, Y., Nonlinear control of magnetic bearing in the presence of sinusoidal disturbance. In Proceedings of the American control conference, Arlington, VA, USA pp. 3636–3641, 2001.

Bishop, R. E. D., and Johnson, D. C., 1960, *The Mechanisms of Vibration*, Cambridge University Press.

Chen K., Tung P., Tsai M. Fan Y., A self tuning fuzzy PID-type controller design for unbalance compensation in an active magnetic bearing, Expert Systems with Applications vol.36 pp.8560-8570, 2009.

Cole, M. O.; Keogh, P. S.; Sahinkaya, M. N.; Burrows, C. R., Towards fault-tolerant active control of rotor-magnetic bearing systems. *Control engineering Practice*, Oxford, v. 12, p. 491-501, 2004.

Elliott, S. J., Stothers, I. M., and Nelson, P. A., ''A Multiple Error LMS Algorithm and Its Application to the Active Control of Sound and Vibration,'' IEEE Trans. Acoust. Speech, Signal Process, 35, pp. 1423-1434, 1987.

Fuller, C.R.; Elliot, S.J.; Nelson, P.A. Active control of vibration. London: Academic Press, 1996.

Johnson, M. E.; Nascimento, L. P.; Kasarda, M. E.; Fuller, C. R., "The effect of actuator and sensor placement on the active control of rotor unbalance", Journal of Vibration and Acoustics, Vol. 125, pp. 365-373, 2003.

Lévine, J., Lottin, J., & Ponsart, J. C., A nonlinear approach to the control of magnetic bearings. IEEE Transactions on Control Systems Technology, 4(5), pp.524-544, 1996.

Maslen E., "Magnetic bearings", University of Virginia, Department of Mechanical, Aerospace, and Nuclear Engineering, Charlottesville, Virginia, USA, June, 2000.

Perini, E. A.; Nascimento, L. P. Análise da força de controle em máquinas rotativas segundo suas frequências críticas utilizando atuadores magnéticos ativos. *In: V Congresso Nacional de Engenharia Mecância,* Salvador, BA. p. 1-11, 2008.

Queiroz, M. S., & Dawson, D. M., Nonlinear control of active magnetic bearings: A backstepping approach. IEEE Transactions on Control Systems Technology, 4(5), 545–552, 1996.

Shi, J.; Zmood, R.; QIN, L. Synchronous disturbance attenuation in magnetic bearing systems using adaptive compensating signals. *Control Engineering Practice*, Oxford, v.12, p.283-290, 2004.

Smith, R. D., & Weldon, W. F., Nonlinear control of a rigid rotor magnetic bearing system: Modeling and simulation with full state feedback. IEEE Transactions on Magnetics, 31(2), 973–980, 1995.

Torres, M., Sira-Ramirez, H., & Escobar, G., Sliding mode nonlinear control of magnetic bearings. In Proceedings of the IEEE international conference control applications, Kohala Coast-Island, Hawaii, USA pp. 743–748, 1999.

Widrow, W., & Stearns, S. D. (1985). Adaptive signal processing, Prentice-Hall Signal Processing Series. Englewood Cliffs, NJ: Prentice-Hall Inc. 07632.

10. RESPONSIBILITY NOTICE

The authors are the only responsible for the printed material included in this paper.